Article:
Patel, H., Routoula, E. and Patwardhan, S.V. orcid.org/0000-0002-4958-8840 (2022) Decontamination of anthraquinone dyes polluted water using bioinspired silica as a sustainable sorbent. Silicon, 14 (3). pp. 1235-1245. ISSN 1876-990X

https://doi.org/10.1007/s12633-020-00851-1

Decontamination of Anthraquinone Dyes Polluted Water Using Bioinspired Silica as a Sustainable Sorbent

Hinesh Patel,[a+] Eleni Routoula[+] and Siddharth V. Patwardhan*
Department of Chemical and Biological Engineering,
University of Sheffield
Mappin Street, Sheffield, UK, S1 3JD
*s.patwardhan@sheffield.ac.uk
[a] Present address: BOC Gases, Whitbty Road, Brislington, Bristol BS4 3QH.
[+] These authors contributed equally.

Abstract

The increased release of harmful dyes in water, along with the continuous reduction of the world's freshwater supplies has placed the textile industry under greater pressure to safely and effectively treat wastewater effluents. Resistance of reactive dyes to breakdown naturally has highlighted the need for specialised removal methods. The growing need for low-cost, efficient sorbents has led to the exploration of bioinspired silica (BIS) due to their green synthesis, proven scalability, and versatility for chemical functionalisation required for dye scavenging. Through a systematic approach, the removal of Reactive Blue 19 from water was studied using a range of BIS, and was compared to removal using a commercial sorbent. While 0% removal was denoted for the commercial sorbent, BIS showed up to 94% removal. The results obtained from a kinetic study suggested a pseudo-second-order reaction, indicating a chemisorption process via electrostatic interactions. Examination of the effects of various adsorption conditions (temperature, pH, sorbent and dye concentrations) using isotherm models (Langmuir and Freundlich) indicated that adsorption was of both chemical and physical nature. Examination of the adsorption mechanism suggest that dye adsorption on BIS was spontaneous. BIS showed higher adsorption capacity (334 mg g^{-1}) compared to literature examples, with rapid adsorption under acidic conditions, excellent thermal stability and a good reuse potential. These findings highlight the potential of BIS as a sustainable, efficient and low-cost sorbent that could be brought forward for future implementation.

Keywords: environmental engineering; green nanomaterials; secondary pollution

Introduction

Industrially, there are approximately 10,000 dyes used within areas such as textiles, cosmetics, food and paper.[1] Their high solubility in water, vibrant colours and ability to withstand light and washing have made dyes applicable within many industries, while their primary utilisation is in the textile industry. As a result, the textile industry has been identified as the second largest wastewater polluting industry in the world.[2] Dye contamination with less than 1 mg L^{-1} of dye would discolour the water, reducing its aesthetic quality, thus making it unsuitable for consumption[3]. To date, an estimated 200,000 tonnes of water are released annually as liquid effluents containing dyes, which is unsustainable, especially given the millions of people that are without safe water supplies or sufficient sanitation.[4]

The health implications associated with the release and contact of dye effluents in the environment have made the need to identify efficient removal techniques even more important. Dye effluents discharged into lakes and rivers can diversely affect their ecosystem, making them inhabitable for fish and other marine organisms due to their toxicity. Other effects are relevant to the disruption of the reproductive system, brain and central nervous system[5], whilst some dyes have carcinogenic and mutagenic effects on living organisms[6]. In addition, dyes can reduce light transmission and increase the chemical oxygen demand in lakes and rivers, reducing photosynthetic activity and promoting oxygen deficiency[7]. A bigger concern is that synthetic dyes are non-biodegradable, and so refrain from being broken down naturally under the influence of sunlight, water or oxidising agents[6]. As a result, the European Union (Directive 2008/1/EC) has placed greater pressure on the textile industry by tightening its legislations, thereby making them responsible for preventing and reducing pollution from the release of effluents[8].

The second largest dye category used within the industry, after azo dyes, is anthraquinone dyes, known best for their reinforced, anthraquinone-based structure, resulting in bright colours and resistance to degradation[9]. As a result these dyes have become harder to break

down than azo dyes[10], whilst their lower fixation – relative mostly to reactive anthraquinone dyes – has led to a significant amount being released into the environment as effluents. Despite their prevalence, removal of anthraquinone dyes has not been given due attention. [11] We recently reviewed the literature on several physical, chemical and biological methods to optimise dye decontamination of dyestuff effluents[11] and found that despite the advantages of many treatment methods, (summarised in Table S1), disadvantages such as high cost, sludge production, and low removal efficiencies have ultimately hampered their implementation on a larger scale.

Adsorption however, has received significant attention towards dye decontamination due to its lower initial costs, flexibility, and ease of operation compared to other techniques. The efficiency of an adsorption process is dependent on whether a sorbent displays high capacity, fast adsorption rates and efficient regeneration. Over the years, activated carbon (AC) has shown promise as an adsorbent for dye removal due to its high surface area and stability[12]. However, widespread use of AC is restricted due to its high costs, as sorbent regeneration is expensive and could potentially lead to a loss of sorbent[13] and a reduction in process efficiency.[5] Zeolites are another class of commonly studied adsorbents for dye removal,[14,15] however, due to being expensive and suffering from regeneration like AC, their industrial implementation is limited.[16]

Research has in recent times turned its attention to silica as an alternate class of sorbents to overcome the aforementioned disadvantages. Silica gel (a microporous sorbent, pores <2nm) is widely known for its high mechanical stability and it exhibits a high surface area enabling it to adsorb large quantities of dye.[17] Furthermore, silica offers the potential of cheaper and more efficient regeneration compared to zeolites and AC, requiring a regeneration temperature of 150^{o}C, compared to 350^{o}C and 200^{o}C for zeolites and AC respectively.[18] However, microporous silica gel creates diffusional challenges when considering high throughput water treatment, or when removing bulky pollutant molecules such as dyes. In order to address this challenge, mesoporous silicas such as MCM-41 and SBA-15 have been

introduced, which have monodisperse, narrow and tunable pores. Given the larger pore sizes, they offer a platform for functionalisation and creation of suitable adsorption sites for a given pollutant, yet without creating significant diffusional limitations. There are numerous examples reported of the use of mesoporous silicas for selective removal of pollutants from water (extensively reviewed in the literature [19-21]). However, these materials are generally prepared under unsustainable conditions and require long synthesis procedures, e.g., elevated temperature, high pressure, strongly alkaline or acidic solutions, with preparations taking several days, thereby making their large-scale production prohibitive.[22] Another major drawback of these materials is the environmentally damaging conditions/ chemicals involved in their production, which lead to secondary pollution – this only shifts the pollution problem. Hence, greener and sustainable alternatives to such porous materials are required.

It appears that diatoms (microalgae) produce large quantities of porous, hierarchically ordered and nanostructured biosilica, entirely under environmentally friendly conditions with remarkable regulation, which is achieved by the use of biomolecules (e.g. proteins, polysaccharides and small amines).[23] The understanding of the roles these biomolecules play *in vivo* has led to the invention of *in vitro* bioinspired silica (BIS) synthesis processes that adopt mild (green) conditions by utilising analogues of biomolecules, called “additives”.[23] The synthesis of bioinspired silica takes 5-15 minutes at neutral pH, in water and room temperature. In contrast to many sorbents (zeolites, mesoporous silicas, and membranes), BIS are sustainable and scalable. Further, technoeconomic evaluation of BIS manufacturing has shown that they are economically viable for industrial scale production in the quantities of sorbents that are typically required for water treatment.[22,24] By controlling the porosity and the surface chemistry, we have demonstrated that bioinspired silicas have exciting opportunities for applications in biomedical, environmental and catalysis areas.[25-27] Utilising this knowledge, bioinspired silica has been tested recently for the extraction of formaldehyde vapour from contaminated indoor air[27] as well as toxic metals from polluted water.[28,29] The

material was shown to provide an excellent alternative to conventional mesoporous silicas but without the attendant secondary pollution that is often encountered.

In this study we aim to systematically evaluate for the first time bioinspired silica as a viable candidate for the removal of Remazol Brilliant Blue R (RB19) from contaminated water. RB19 was chosen as it is an important anthraquinone dye, representing a recalcitrant category of dyes. It is also a commonly investigated dye in the literature, thus allowing a wider comparison. Specifically, we aim to use three types of BIS (PS7, PS5 and PS2) containing a decreasing amount of amine functionalisation, engineered via the synthesis process recently reported.[30] Although these materials were extensively characterised in that paper,[30] this is the first report of examining BIS application in the removal of organic pollutants from water. Our previous study reported an oxide composite of Si and Fe which was applied for arsenic removal,[28] but their structures, properties, composition and interactions with arsenic were fundamentally different compared to RB19 studied herein. In order to provide a clear comparison, we will use a commercial porous silica as a benchmark for adsorptive removal. We aim to provide mechanistic understanding of the performance of BIS through a combination of extensive analysis of the adsorption kinetics and isotherms, and the regeneration of sorbents; as extensive materials characterisation has been reported elsewhere [29], the focus of this work is on adsorptive removal of RB19. It is hoped that this study will help identify sorbent systems which could pave the way for a more economically feasible dye removal process, and will open the door for optimisation of these conditions, with the potential to scale up.

Materials and Methods

Chemicals and Reagents

All chemicals used were of analytical reagent grade and used as received from the suppliers. Deionised water was used to prepare aqueous solutions and for washing post-centrifugation. Technical grade sodium metasilicate pentahydrate and hydrochloric acid were obtained from Fisher Scientific and technical grade pentaethylenehexamine (PEHA) and Reactive Blue 19

were obtained from Sigma–Aldrich. Reactive Blue 19 (RB19) or Remazol Brilliant Blue R is an anthraquinone dye (Figure 1) and used as a model pollutant herein. Upon dissolution in deionised water, the pH of RB19 becomes circumneutral to slightly acidic. Commercial porous silica, Syloid-AL1FP was kindly supplied by Grace Silica GmBH.

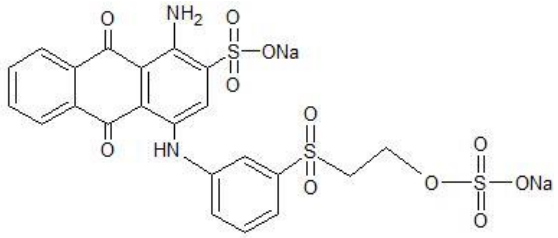

Figure 1: Chemical structure of Reactive Blue 19.

Bioinspired Silica (BIS) Synthesis and Characterisation

In this study, BIS synthesis was achieved using pentaethylenehexamine (PEHA) as an additive and sodium silicate as the silica precursor, following an established method published elsewhere.[31] Two separate solutions of sodium metasilicate and PEHA were prepared in deionised water before mixing them together (final [Si] = 30mM and [Si] **:** [N] = 1). Following this, the mixture was rapidly neutralised to pH7 using 1 M hydrochloric acid.[31] Neutralisation of the silicate solution in the presence of this amine promoted rapid silica formation, resulting in BIS nanoparticles with PEHA occluded inside and on surface. Upon completion of the reaction (5 min), further addition of acid was used to controllably remove amine from the BIS nanoparticles. Amine removal can be controlled through the final pH of the solution, achieving no amine removal (at pH7, as synthesised), partial removal (at pH5) or complete removal (at pH2), the latter being equivalent to calcination.[30] The samples were then isolated via three consecutive cycles of centrifugation and washing with deionised water. Solids were dried in an oven overnight at 80°C prior to materials characterisation and use in adsorption tests. In order to probe information on surface areas and porosities, the dried samples were subjected to porosimetry analysis via N_2 adsorption, using Micromeritics ASAP 2420 as reported previously.[30]

RB19 Adsorption

A stock solution of 75 mg L^{-1} RB19 was prepared by dissolving a specific amount of powdered RB19 into deionised water using a magnetic stirrer for 5 minutes. A stock solution of sorbent was also prepared by suspending 10 g L^{-1} of a known sorbent (PS7, PS5, PS2 or Syloid-AL1FP) into deionised water under sonication for 5 minutes, to ensure effective dispersion. Immediately prior to the adsorption tests, freshly prepared sorbent dispersions were mixed using a vortex at 1200 rpm for 30 seconds and desired concentration were prepared by diluting the stock solution. Samples were prepared by pipetting 1 mL of RB19 and 1 mL of sorbent solution into 2 mL Eppendorf tubes and mixed using a vortex for 15 seconds to allow the dye and sorbent solutions to effectively mix together.

Adsorption kinetics were studied as follows. 2mL samples in closed Eppendorf tubes were incubated in a shaking water bath (25ºC, 180 rpm) and were removed and analysed over regular time intervals until no further change of dye concentration was observed. Separate samples were used for each time point. A maximum 7-day profile was considered in order to clearly understand and distinguish the adsorption mechanisms. Extracted samples were centrifuged at 10,000 rpm for 5 minutes and supernatant was analysed using a Genesys 10S UV-vis spectrophotometer (absorbance measured at λ_{max} = 595 nm and converted to concentration using a pre-determined calibration curve, see S.I.). The adsorption capacity (q_t, mg g^{-1}) and removal efficiency (*RE*, %) of each sorbent was determined through the following equations:

$$\mathbf{q_t} = \frac{(\mathbf{C_0} - \mathbf{C_e})(\mathbf{V})}{\mathbf{w}} \quad (1)$$

$$\mathbf{RE} = \frac{C_0 - C_e}{C_0} \text{ x } 100 \quad (2)$$

where C_0 and C_e are the initial and equilibrium concentration of RB19 in the solution (mg L^{-1}), V is the volume of solution (L) and w is the mass of the sorbent (g).

In order to obtain adsorption isotherms, a stock solution of 1500 mg L^{-1} RB19 was prepared and used to produce dye-sorbent samples at different initial dye concentrations (C_0, mg L^{-1}) ranging from 12.5 to 1500 mg L^{-1}. A maximum concentration of 1500 mg L^{-1} was considered based on the strong adsorption performances of PS5 and PS7 and also because some dyes are highly toxic to aquatic life at high concentrations (500-1000 mg L^{-1}). The adsorption tests were performed as described above. The samples were allowed the optimum contact time identified from the kinetic study for each sorbent, which were 4-days for Syloid-AL1FP, and 7-days for PS2, PS5 and PS7.

Further analysis was conducted for the best performing samples as identified from the adsorption study, in order to identify the optimal pH and temperature. For these experiments, stock solutions of RB19 (initial dye concentration of 75 mg L^{-1}) and sorbent (initial concentration of 10 g L^{-1}) were prepared, using deionised water as solvent and regulating solution pH using HCL, 1M and NaOH 1M between pH 3 to pH 11. As described above, 1 mL of RB19 and 1 mL of sorbent solutions, both of same pH, were mixed into 2 mL Eppendorf tubes, incubated in a water bath and the residual concentration of RB19 was measured at pre-determined time intervals. The same procedure was repeated over 20°C (room temperature), 30°C and 50°C for the optimal pH for the solutions as identified above. Furthermore, a study on the effect of quantity of BIS present during adsorption was conducted. Keeping the pH, temperature and initial RB19 concentration constant (75 mg L^{-1}), the concentration of sorbent present in the mixture was varied from 0.5 g L^{-1} to 10 g L^{-1} (concentration in final mixture). Samples were prepared as described previously and residual concentration of RB19 was measured in pre-determined time intervals as described above.

Results and Discussion

Materials Characterisation

The porosity and composition data for the samples, as obtained from nitrogen adsorption analysis is shown in Table 1. The commercial silica, Syloid, had moderate surface area and is predominantly a mesoporous material with high pore volume. BIS samples seem

microporous with low to medium surface areas, while the post-synthetic acid washing step enabled a gradual increase in surface area and controlled functionalisation, agreeing with our previously published results.[30] BIS pH 7 (PS7) had the lowest surface area and the highest additive content remaining, where additive is located on the outer and inner surface. BIS pH 5 (PS5) showed slightly increased surface area and reduced additive content as the additives remain on the inner surface only, while those from external surface were removed. In BIS pH 2 (PS2), there is a complete additive removal, leading to a pure and porous material, equivalent to silica after calcination. As the controlled presence (or absence) of the additive in silica creates different levels of surface functionalisation (and ionisation), these results show that the synthesis method was able to engineer the functionalisation on BIS.

Table 1: Materials characterisation

Property	**Syloid**	**PS7**	**PS5**	**PS2**
Surface area (m^2/g)	307	115	195	480
Pore diameter (nm)	15.8	-- [a]	-- [a]	-- [a]
Pore volume (cm^3/g)	1.42	0.093	0.097	0.122
Organic content (wt%)	0 [b]	14.85[c]	10.85[c]	0[c]

[a] no clear size seen, only a broad distribution; [b] information obtained from the supplier; [c] data used from ref. [30].

RB19 Adsorption Kinetics and Adsorption mechanism

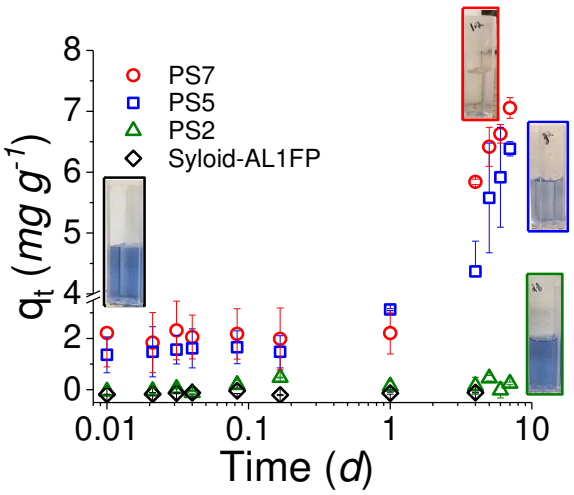

Figure 2: Time dependent uptake of RB19. The insets show photos of samples at the beginning (t≈0) and end of adsorption for various samples (outline colours match the symbol colours).

We investigated the adsorption kinetics by incubating the dye containing solutions with various silica samples and measured the adsorption as a function of time. The amount adsorbed and the visual appearance of the samples examined are shown in Fig. 2. Commercial silica (Syloid-AL1FP) was shown to be ineffective as a sorbent for RB19 uptake. It appears that as both the dye and silica surface would be anionically charged under the adsorption conditions, there were no interactions occurring between them, and hence no apparent dye adsorption occurred. Similar to Syloid-AL1FP, PS2 displayed minimal dye uptake over a 7-day period, indicating that its performance was identical to that of commercial silica. This could be explained by the absence of any functionalisation of PS2 surface (due to a complete removal of the additive), resulting in no interactions between the sorbate and sorbent.

On the other hand, PS5 and PS7 samples displayed a very different performance (which is statistically significant, see S.I. for t-test results). The uptake of RB19 onto PS5 and PS7 is denoted by two phases: (a) a slow initial rate of removal for approximately 4 hours where 20-30% of dye was adsorbed, and (b) a faster rate of adsorption after 1-day. It is likely that the first phase represents the time taken for large dye molecules to diffuse through the smaller pores, while the second phase may represent stronger and faster interactions between the functionalised sorbent surface and the sorbate. The enhancement of dye uptake onto PS5 and PS7 is most likely attributed to electrostatic interactions between the anionic sulfonate groups of the dye and the protonated amino groups on the sorbent. After 7 days, the maximum dye removal achieved was 85% (PS5) and 94% (PS7) while the capacity (q_e) was 6.39 mg g^{-1} (PS5) and 7.06 mg g^{-1} (PS7).

The kinetic evaluation of an adsorption mechanism is critical in determining the rate at which a process occurs, to aid feasibility of scale up operations[32,33]. Given the complexity of the adsorption in this case, which may include effects from porosity, surface chemistry, chemisorption and diffusion, using established models to describe the adsorption kinetics can provide valuable mechanistic information. With this view, the adsorption data obtained for PS5 and PS7 (Syloid-AL1FP and PS2 were omitted as they showed no uptake) were modelled

according to a pseudo-first order[34] (Eqn.5) and a second-order models[35] (Eqn.6), which are commonly used to describe an adsorption process between dye molecules and sorbents[36].

$$q_t = q_e - q_{e,calc} \times e^{-k_1 t} \quad (5)$$

$$\frac{t}{q_t} = \frac{1}{k_2 q_{e,calc}^2} + \frac{1}{q_{e,calc}} t \quad (6)$$

where k_1 (day^{-1}) is the pseudo-first-order rate constant, q_e and q_t (mg g^{-1}) are the adsorption capacities at equilibrium and time t respectively, k_2 (g mg^{-1} day^{-1}) is the second order rate constant and $q_{e,calc}$ (mg g^{-1}) is the modelled equilibrium capacity. For the second-order kinetics, the initial rate of adsorption (h, mg g^{-1} day^{-1}) can be calculated using Eqn.7:

$$h = k_2(q_{e,calc}^2) \quad (7)$$

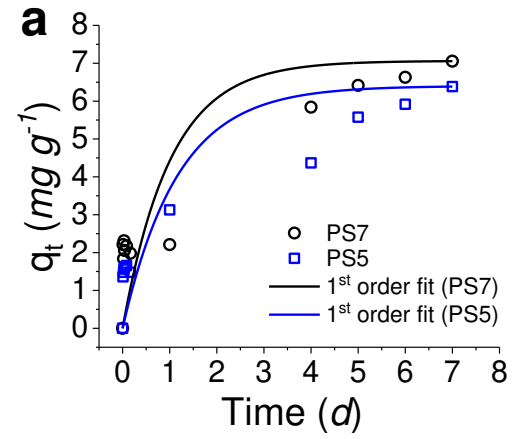

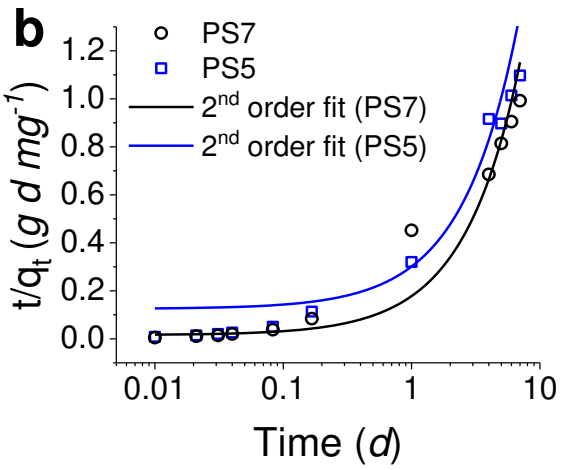

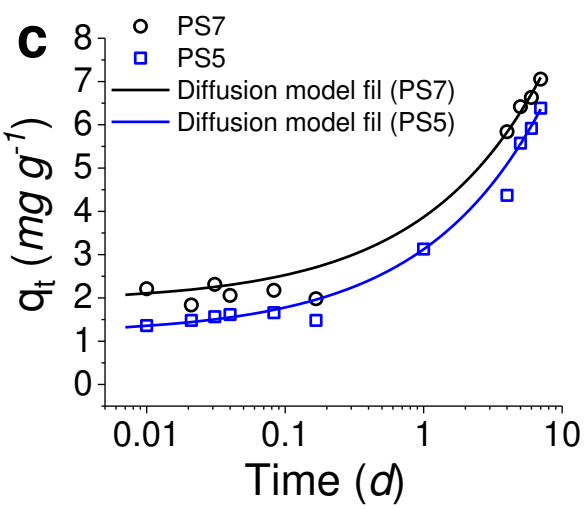

Figure 3: Regression analysis of the adsorption kinetics of RB19 onto PS5 and PS7 using (a) a pseudo-1st order model, (b) and 2nd order model and (c) an intra-particle diffusion model (Weber-Morris). The X-axes in middle and bottom graphs is shown as log-scales in order to provide clarity of the fit especially towards to shorter time data points.

When the adsorption kinetics were analysed using a first-order kinetics model (Eqn.5), it is clear from Figure 3a that the data from either samples (PS5 or PS7) could not be adequately described using this model. This is expected because the first-order kinetic model is most suitable for systems with physisorption on flat or smooth surfaces, while in this case, we have porous materials with potential for chemisorption due to functionalisation. In order to further test this hypothesis, we analysed the data for both samples using a second-order kinetics model, as it accounts for any chemisorption, if present.[36] The corresponding results from a regression analysis are shown in Figure 3b. Note that the X-axis in this graph is shown in log-scale (which is not usual), in order to provide clarity of the fit, especially towards the data points at the lower-end.

From Figure 3 it is clear that PS7 follows second-order kinetics (R^2 = 0.991), thereby providing evidence for chemisorption as the main adsorption mechanism (also see Table 2). Chemisorption occurs via electrostatic interactions between the anionic sulfonate groups from the dye molecules and protonated amines from the additive molecules present on the silica surface. In contrast for PS5, although the second-order kinetics model fits the data partially, it particularly does not describe the adsorption process at shorter time-scales (Figure 3b, R^2 = 0.8255). This suggests that, although the adsorption process may be driven by chemisorption

at a later stage, the early stages of adsorption do not follow a chemisorption model. This observed difference between the PS7 and PS5 samples can be attributed to the differences in the location of the amine functionalisation present on the silica surfaces. Our data has shown that for PS7 samples, amines are present both on the external surface and the internal pores walls (Figure 4 *i*).[30] PS5 is an interesting case where the external surface is "clean" and the amines are only present on the internal pore walls (Figure 4 *iv*). This leads to physisorption on the external surface of PS5 sample (Figure 4 *v*) followed by chemisorption on the internal pores (Figure 4 *vi*), while for PS7, chemisorption is dominating as all available surfaces are amine functionalised (Figure 4 *i-iii*).

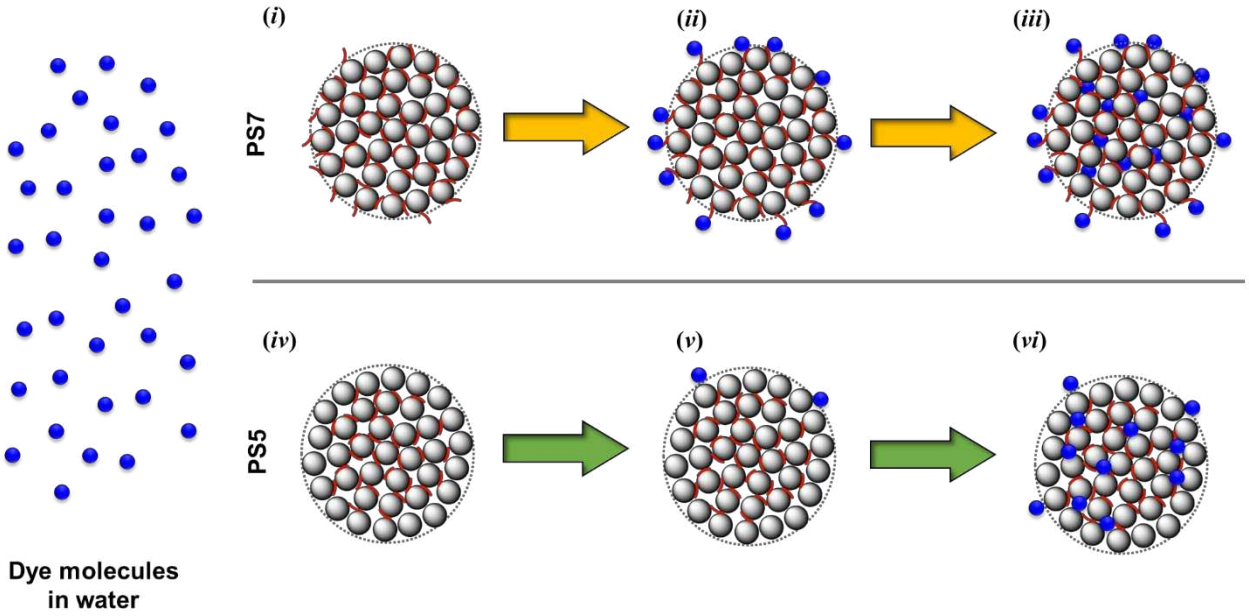

Figure 4: A schematic representation of the adsorption process of RB19 dye (blue dots) on PS7 (top panel, *i*) and PS5 (bottom panel, *ii*). Red lines show the additives (amines) present on silica surfaces (external and/or internal). See text for details.

For porous sorbents with chemisorption, it is more common to exhibit the influence of intra-particle diffusion. This was tested by analysing the kinetics data according to the Weber and Morris model shown in Eqn.8:

$$q_t = k_i t^{0.5} + C_i \quad (8)$$

where k_i is the intra-particle diffusion rate (mg g^{-1} day$^{-0.5}$) and C_i is the boundary layer constant.

The results from the regression analysis are shown in Figure 3c. [Note that the X-axis in this graph is shown in log-scale (which is not usual), in order to provide clarity of the fit especially towards the data points at the lower-end.] The graph shows excellent fits to the data for both samples (with R^2 = 0.9959 for PS5 and 0.991 for PS7, see Table 2). This clearly suggests that, in addition to chemisorption, the diffusion of the dye molecules into the pores of silica particles is a rate determining step.[37,38,3,39] It is interesting to note that the diffusion rate constant k_i for both samples is identical, which suggests that the pores in both samples have similar physical and chemical properties (e.g. size, structure and surface chemistry). This corroborates our earlier findings[30] and the fact that both samples had the same origin, with PS5 undergoing an additional acid wash at pH5 in order to remove only the externally-residing amines and retain the internal functionalisation. We note that this mechanism is fundamentally different to that reported for the removal of arsenic in our previous publication,[28] which reported selective adsorption of arsenic through the formation of mono- and bi-dentate "Fe–As" complex.

Table 2: Kinetic parameters for sorption of RB19 onto PS5 and PS7

Sorbent	**Second Order model**				**Webber-Morris Model**		
	k_2 [a]	$q_{e(calc)}$ [b]	h [c]	R^2	k_i [d]	C_i [b]	R^2
PS5	0.25	5.67	7.99	0.8255	1.96	1.16	0.9969
PS7	1.69	6.16	64.3	0.991	1.96	1.91	0.991

Units: [a] g mg^{-1} d^{-1}; [b] mg g^{-1}; [c] mg g^{-1} d^{-1}; [d] mg g^{-1} $d^{-0.5}$

Adsorption Isotherms

The dye removal by each of the four sorbents was investigated as a function of the initial concentration of the dye present (Figure 5a). Both Syloid and PS2 samples showed around 40-50% dye removal, which was independent of the initial dye concentration. This is interesting because a plateau was not observed, indicating saturation was not reached even at the very high initial dye concentrations used (1500 mg L^{-1}). It is likely that the dye molecules may be clustering on the silica particles, although further work is needed to gain a better

understanding. PS5 and PS7 exhibited high dye removal capacities at lower initial dye concentration (92 and 97% for PS5 and PS7 respectively). These decreased with increasing initial dye concentration, reaching to 44 and 75% respectively for PS5 and PS7. A drop in capacity is expected with the increasing sorbate concentration due to a reduction in available adsorption sites, however, it is worth noting that the dye removal efficiency of PS7 dropped only to 75%, thereby showing excellent potential.

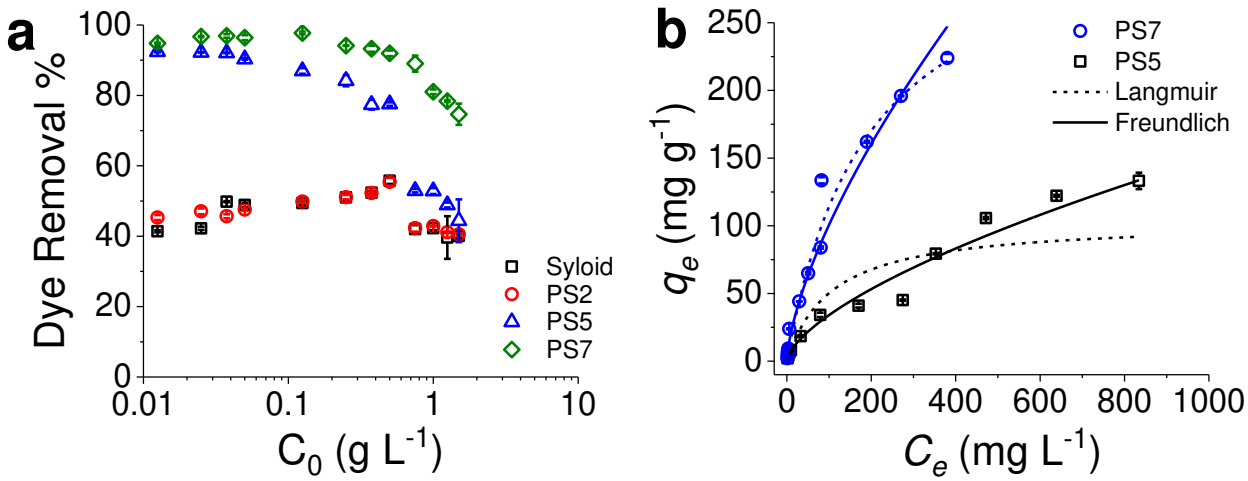

Figure 5: (a) Effect of initial RB19 concentration on dye removal by silica samples. X-axis is log-scale in order to expand the lower-end data points. (b) Langmuir and Freundlich adsorption isotherms for RB19 uptake onto PS5 and PS7.

The adsorption isotherms were fitted against the Langmuir and Freundlich models (see Eqn.9 and Eqn.10) to explain the mechanisms governing the sorption of RB19 onto the examined sorbents:

$$\boldsymbol{q_e = \frac{q_m b C_e}{1+bC_e}} \text{ , where } \boldsymbol{R_L = \frac{1}{1+bC_0}} \quad (9)$$

$$\boldsymbol{q_e = K_F C_e^{\frac{1}{n}}} \quad (10)$$

where q_e and q_m are the equilibrium capacity (mg g^{-1}) and the maximum adsorption capacity (mg g^{-1}) of the sorbent respectively, C_e is the equilibrium dye concentration (mg L^{-1}), b is a

Langmuir equilibrium constant, R_L is the separation factor, and K_F and $\frac{1}{n}$ are the Freundlich constants.

The Langmuir isotherm model is used to describe a monolayer surface coverage at specific homogenous sites within an adsorbent and that adsorption can no longer take place at a site once occupied by a dye molecule[40]. The Langmuir model can be additionally used to describe a chemisorption mechanism [3]. The non-linearised form of the Langmuir isotherm model and its separation factor (R_L), used to indicate the affinity of the sorbent towards the sorbate, can be represented by Eqn.9 [41]. The condition of $0 < R_L < 1$ indicates favourability towards adsorption. The Freundlich isotherm model (Eqn.10), unlike the Langmuir model, assumes multilayer adsorption on a heterogeneous surface and that adsorption can still occur at an already occupied site.[42] $1/n$ is used to indicate the affinity and hence favourability of the sorbent towards the sorbate: $0 < 1/n < 1$ indicates strong interactions between RB19 and the respective sorbent and hence also indicating favourability[3].

The experimental data for RB19 uptake onto PS2 and Syloid-AL1FP did not provide a definitive fit to either the Langmuir or Freundlich models (not shown), hence these two samples were not analysed further. Fitting the experimental adsorption isotherms for RB19 uptake onto PS5 and PS7 showed that while the data from both samples were well represented by the Freundlich model, only PS7 followed the Langmuir model (Table 3 and Fig. 5b). In the case of PS7, the observed higher adsorption affinity (see K_F values in Table 3), a good fit with Langmuir model and a higher maximum capacity (q_m) when compared to PS5 sample strongly support the presence of chemisorption through electrostatic interactions identified from the second-order kinetics model.

Table 3: Parameters of adsorption isotherm models.

Sorbent	Langmuir			Freundlich		
	q_m [a]	b [b]	R^2	$1/n$	K_F [c]	R^2
PS5	103*	0.009*	0.895*	0.65	1.74	0.966
PS7	334	0.005	0.995	0.67	4.56	0.997

Units: [a] mg g^{-1}, [b] L mg^{-1}, [c] $mg^{1-1/n}$ $L^{1/n}$ g^{-1}

** Due to a poor fit for PS5 with Langmuir model, these values are shown for completeness and they should not be used to draw quantitative inferences.*

The maximum adsorption capacity of RB19 onto PS7 silica was compared against some of the best performing adsorbents reported in literature (see Table 4). The adsorption capacity of PS7 reported in this study (334 mg g^{-1}) is significantly higher than the highest capacity reported previously for any sorbent (250 mg g^{-1}[43] and 221 mg g^{-1}[43]), and it is an order of magnitude higher than most competing sorbent materials. Additionally, excellent removal efficiencies were observed for PS7 for dye concentrations as high as 1500 mg L^{-1} (see Figure 3), which surpass those reported in the literature.[44,6,14] These results highlight that bioinspired silica can be extensively used to remove high concentrations of RB19 that are likely to pose greater environmental and health concerns.

Table 4: Comparison of sorption performance for RB19 uptake with competing sorbents reported from literature

Sorbent	***q_m*** ***(mg g^{-1})***	**Optimum Conditions**	**Ref**
PS7	**334**	25ºC, pH7 of dye, 0-400 mg L^{-1}	This Study
Powdered AC	52	25ºC, pH 2.0, 60 mg L^{-1}	[45]
Modified Clinoptilolite	42	35ºC, pH 6.0, 250 mg L^{-1}	[14]
NiO Nanoparticles	99	45ºC, pH 6.5, 75 mg L^{-1}	[6]
Scallop shell	250	25 ºC, pH 6, 100mg L^{-1}	[44]
Rice straw fly ash	221	60ºC, pH 1.0, 30 mg L^{-1}	[43]
Nanohydroxyapetite	90	20ºC, pH 3, 100 mg L^{-1}	[46]
Natural Orange Peel	25	30ºC, pH 4.0. 300 mg L^{-1}	[47]
Sodium Hydroxide treated orange peel	46	30ºC, pH 4.0. 300 mg L^{-1}	[47]
Sodium alginate/poly(*N*-vinyl-2-pyrrolidone) blend hydrogel	55	25ºC, pH 1.2, 300 mg L^{-1}	[48]
Silica gel with 2,2'-(pentane-1,-5-diylbis (oxy))dibenzaldehyde	55	55ºC, pH 5, up to 40mg L^{-1}	[49]
Acetic acid treated biosorbent from *Citrus sinensis*	75	30ºC, pH 2, up to 300mg L^{-1}	[50]
Heat-inactivated biomass on alginate beads	48	30ºC, pH 2, 150mg L^{-1}	[51]

Optimisation of adsorption conditions

Although PS7 exhibited a significantly higher capacity than any other adsorbent reported to date, the adsorption was slow. In order to optimise the adsorption rate, the effect of pH on dye removal was examined for the best-performing sorbent (PS7) over a range from pH3 to pH-11 (Figure 6a). Results indicated that the optimal pH value for RB19 removal through adsorption on bioinspired silica is in the range between pH 3 and pH 7. This is consistent with the literature (see Table 4), where it has been reported that acidic conditions are favoured for the adsorption of RB19because the dye remains anionic at most pH considered due to its strong sulfonic acid moieties (low pk_a), while the sorbents gradually deprotonate with increasing pH. This results in stronger interactions between the dye and PS7 at low pH, which rapidly weaken for pH>7. Further analysis of the adsorption kinetic profile for two selected pH values (3 and 5), revealed that the kinetics of adsorption are spectacularly fast at pH3 (see Figure 6b compared to the data in Figure 2). Nearly 90% of dye was removed at pH3 before the first reading was taken at 30 min. This high rate of adsorption under optimised conditions coupled with a very high capacity makes PS7 a most promising candidate for future implementation.

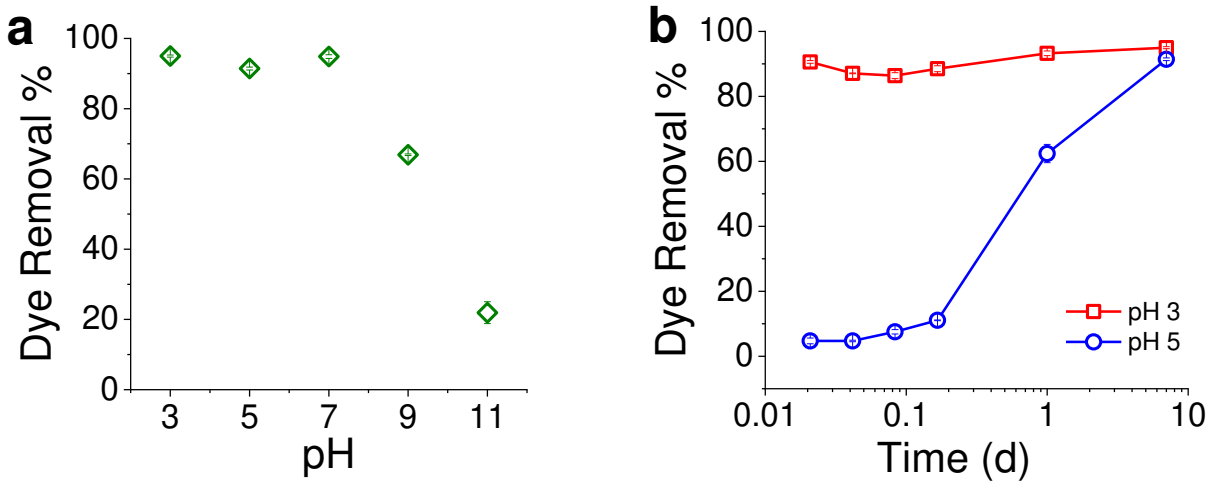

Figure 6: (a) The effect of pH on RB19 adsorption on bioinspired adsorbent PS7. (b) Kinetic study of the effect of pH 3 and pH 5 on RB19 adsorption on bioinspired adsorbent PS7.

The effect of adsorbent dosage was examined next by varying PS7 concentration from to 0.5 to 10 g L^{-1}, and using optimised conditions (dye concentration at 75 mg L^{-1}, solution pH at 3

and temperature at 20ºC). Over the adsorbent dosage used, the amount of dye removed remained in the range of 92-95% over 24 hours (Figure 7a). Further, we examined the adsorption kinetics for different sorbent dosage (Figure 7b). It is clear that within the first 10 min the majority of dye has already been adsorbed on the sorbent, regardless of the sorbent quantity present in the solution. These results are encouraging because it is clear that the adsorbent is not saturating under the conditions, which is also consistent with the literature.[46]

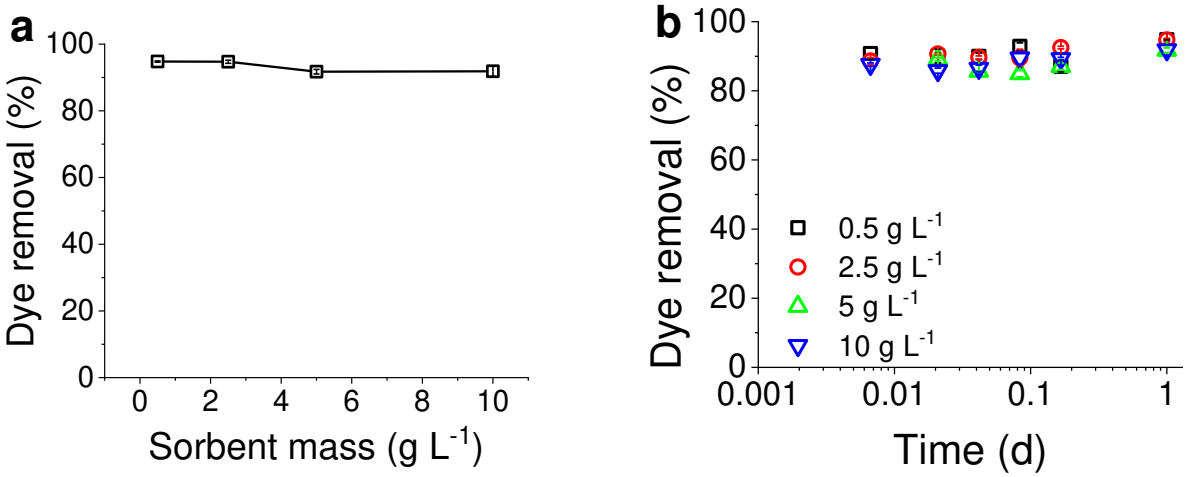

Figure 7: (a) Effect of PS7 mass on the adsorption of RB19 over a 24h incubation period. (b) Effect of PS7 mass on the adsorption of RB19 over time (X-axis is log-scale in order to expand the low-end data points).

Finally, keeping all other parameters constant (RB19 concentration at 75 mg L^{-1}, pH 3, PS7 dosage at 5 g L^{-1}), we examined the effect of temperature over the course of 7 days (Fig 8). Samples at 20ºC seem to perform better at the beginning (30 min time point) compared to adsorption at 30ºC and 50ºC. However, these differences gradually diminish over time and PS7 removed a similar amount of dye over the range of temperatures studied, thus suggesting a good stability over the temperature range examined. While in the literature both increase and decrease in dye removal has been reported with increased temperature,[49,43,50,46] it is clear that the nature of the adsorbent, in particular its surface chemistry, controls this behaviour. PS7, as discussed above, is heavily functionalised with amines (see Table 1) and at the adsorption conditions (pH3), the surface will be highly protonated. This leads to strong ionic bonding between the dye (which is anionic, see above) and the cationic PS7, which does not

seem to be affected by temperature within the range studied herein. Further, preliminary results from the regeneration of the adsorbents (see S.I.) show a high potential of PS7 regeneration and reuse.

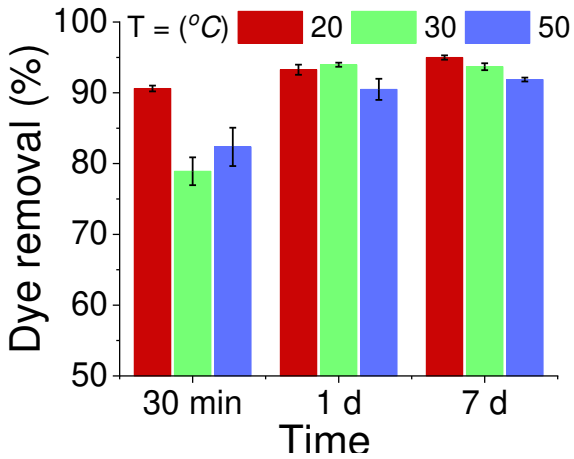

Figure 8: Effect of temperature on the adsorption of RB19 over 7 days.

Conclusion

This study reports the first use of bioinspired silicas (BIS) for the removal of a representative anthraquinone dye (RB19) from polluted water. By systematically controlling the synthesis procedure, we produced samples with varying amine functionality and compared their performance against a commercial porous silica. Bioinspired silica with full (PS7) or partial (PS5) amine presence exhibited high RB19 uptake capacities; PS7 showing the highest capacity reported to date. Through extensive analysis of the adsorption kinetics and isotherms, it was found that adsorption was highly favourable and that more than one mechanism controlled the overall process. In particular, we identified that intra-particle diffusion of the dye into the porous structures, as well as chemisorption of dye onto the amine sites via electrostatic interactions were the main mechanisms involved. As a result of these strong interactions, PS7 was able to maintain the performance even at very high dye concentrations that are usually found in “real” effluents. Optimisation of conditions further revealed that PS7 is a robust adsorbent, offering fast uptake at acidic pH, with very high dye removal efficiencies.

Further, PS7 was stable over a range of temperatures with the potential to reuse. Overall this study identified the promising potential of bioinspired silica as an efficient and robust dye sorbent for wastewater treatment which is very easy to synthesise and is environmentally friendly, thereby making it an excellent candidate for further studies and implementation in decontamination applications.

Acknowledgements

The authors thank the Department of Chemical and Biological Engineering at the University of Sheffield for the financial support.

References

1. Bharathi K, Ramesh S (2013) Removal of Dyes Using Agricultural Waste as Low-Cost Adsorbents: A Review. Applied Water Science 3:773-790

2. Sostar-Turk S, Simonic M, Petrinic I (2005) Wastewater Treatment After Reactive Printing, Dyes and Pigments. Dyes and Pigments 64 (2):147-152

3. Elwakeel K, El-Binday A, Ismail A, Morshidy A (2016) Sorptive Removal of Remazol Brilliant Blue R from Aqueous Solution by Diethylenetriamine Functionalized Magnetic Macro-Reticular Hybrid Material. RSC Advances 6 (27):22395 - 22410

4. Tebbutt T (1998) Principles of Water Quality Control. 5th edn. Butterworth-Heinemann,

5. Salleh M, Mahmoud D, Karim W, Idris A (2011) Cationic and Anionic Dye Adsorption by Agricultural Solid Wastes: A Comprehensive Review. Desalination 280 (1-3):1 - 13

6. Monshef Khoshhesab Z, Ahmadi M (2015) Removal of Reactive Blue 19 from Aqueous Solutions Using NiO Nanoparticles: Equilibrium and Kinetic Studies Desalination and Water Treatment 57 (42):20037 - 20048

7. Assadi A, Nateghi R, Reza Bonyadinejad G, Mehdi Amin M (2012) Decolorization of Direct Poly Azo Dye with Nanophotocatalytic UV/NiO Process. International Journal of Environmental Health Engineering 1 (3):1-5

8. Gomez J, Galan J, Rodriguez A, Walker G (2014) Dye Adsoprtion onto Mesoporous Materials: pH Influence, Kinetics ad Equilibrium in Buffered and Saline Media. Journal of Environmental Management 146:355-361

9. Banat I, Nigam P, Singh D, Marchant R (1996) Microbial Decolourization of Textile Dye Containing Effluents: A Review. Bioresource Technology 58 (217-227)

10. Lee Y, Matthews R, Pavlostathis S (2005) Biological Decolourization of Reactive Anthraquinone and Phthalocyanine Dyes Under Various Oxidation-Reduction Conditions Water Environment Research 78 (2):156-159

11. Routoula E, Patwardhan SV (2020) Degradation of Anthraquinone Dyes from Effluents: A Review Focusing on Enzymatic Dye Degradation with Industrial Potential. Environ Sci Technol 54 (2):647-664

12. Aljeboree A, Alshirifi A, Alkaim A (2014) Kinetics and Equilibrium Study for the Adsorption of Textile Dyes on Coconut Shell Activated Carbon. Arabian Journal of Chemistry 10 (2):S3381-S3393

13. Qu J (2008) Research Progress of Nove Adsorption Processes In Water Purification: A Review. Journal of Environmental Sciences 20:1-13

14. Alrozi R, Anuar N, Senusi F, Kamaruddin M (2016) Enhancement of Remazol Brilliant Blue R Adsorption Capacity by Using Modified Clinoptilolite. Iranica Journal of Energy and Environment 7 (2):129 - 136

15. Wang S, Li H, Xu L (2006) Application of Zeolite MCM-22 for Basic Dye Removal from Wastewater. Journal of Colloid and Interface Science 295 (1):71 - 78

16. Bhatnagar A, Minocha A (2006) Conventional and Non-Conventional Adsorbents for Removal of Pollutants from Water - A Review. Indian Journal of Chemical Technology 13:203 - 217

17. Crini G (2006) Non-Conventional Low-Cost Adsorbents for Dye Removal: A Review. Bioresource Technology 97 (9):1061 - 1085

18. Yang R (2003) Adsorbents: Fundamentals and Applications. In., 1st Edition edn. John Wiley & Sons, pp 131-132

19. Diagboya PNE, Dikio ED (2018) Silica-based mesoporous materials; emerging designer adsorbents for aqueous pollutants removal and water treatment. Micropor Mesopor Mat 266:252-267. doi:10.1016/j.micromeso.2018.03.008

20. Gibson LT (2014) Mesosilica materials and organic pollutant adsorption: part B removal from aqueous solution. Chem Soc Rev 43 (15):5173-5182. doi:10.1039/c3cs60095e

21. Walcarius A, Mercier L (2010) Mesoporous organosilica adsorbents: nanoengineered materials for removal of organic and inorganic pollutants. Journal of Materials Chemistry 20 (22):4478-4511. doi:10.1039/B924316J

22. Patwardhan SV, Manning JRH, Chiacchia M (2018) Bioinspired synthesis as a potential green method for the preparation of nanomaterials: Opportunities and challenges. Curr Opin Green Sust 12:110. doi:10.1016/j.cogsc.2018.08.004

23. Patwardhan SV, Staniland SS (2019) Green Nanomaterials. From bioinspired synthesis to sustainable manufacturing of inorganic nanomaterials. IOP Publishing doi:10.1088/978-0-7503-1221-9

24. Drummond C, McCann R, Patwardhan SV (2014) A feasibility study of the biologically inspired green manufacturing of precipitated silica. Chemical Engineering Journal 244:483-492. doi:10.1016/j.cej.2014.01.071

25. Forsyth C, Patwardhan SV (2013) Controlling performance of lipase immobilised on bioinspired silica. J Mater Chem B 1 (8):1164-1174. doi:10.1039/c2tb00462c

26. Davidson S, Lamprou DA, Urquhart AJ, Grant MH, Patwardhan SV (2016) Bioinspired Silica Offers a Novel, Green, and Biocompatible Alternative to Traditional Drug Delivery Systems. Acs Biomaterials Science & Engineering 2 (9):1493-1503. doi:10.1021/acsbiomaterials.6b00224

27. Ewlad-Ahmed AM, Morris MA, Patwardhan SV, Gibson LT (2012) Removal of Formaldehyde from Air Using Functionalized Silica Supports. Environ Sci Technol 46 (24):13354-13360. doi:10.1021/es303886q

28. Alotaibi KM, Shiels L, Lacaze L, Peshkur TA, Anderson P, Machala L, Critchley K, Patwardhan SV, Gibson LT (2017) Iron supported on bioinspired green silica for water remediation. Chemical Science 8 (1):567-576. doi:10.1039/C6SC02937J

29. Arkas M, Tsiourvas D (2009) Organic/inorganic hybrid nanospheres based on hyperbranched poly(ethylene imine) encapsulated into silica for the sorption of toxic metal ions and polycyclic aromatic hydrocarbons from water. J Hazard Mater 170 (1):35-42. doi:10.1016/j.jhazmat.2009.05.031

30. Manning JRH, Yip TWS, Centi A, Jorge M, Patwardhan SV (2017) An Eco-Friendly, Tunable and Scalable Method for Producing Porous Functional Nanomaterials Designed Using Molecular Interactions. ChemSusChem 10 (8):1683-1691. doi:10.1002/cssc.201700027

31. Manning JRH, Routoula E, Patwardhan SV (2018) Preparation of functional silica using a bioinspired method. Journal of Visualized Experiments:in press

32. Calvete T, Lima E, Cardoso N, Dias S, Pavan F (2009) Application of Carbon Adsorbents Prepared from the Brazilian Pine-Fruit-Shell for the Removal of Procion Red MX 3B from Aqueous Solution - Kinetic, Equilibirum and Thermodynamic Studies. Chemical Engineering Journal 155 (3):627 - 636

33. Feng Y, Zhou H, Liu G, Qiao J, Wang J, Lu H, Yang L, Wu Y (2012) Methylene Blue Adsorption onto Swede Rape Straw (Brassica Napus L) Modified by Tartaric Acid: Equilibrium, Kinetic and Adsorption Mechanism. Bioresource Technology 125:138 - 144

34. Lagergren S (1898) About the Theory of So-Called Adsorption of Soluble Substances Kungliga Svenska Vetenskapsakademiens Handlingar 24:1-39

35. Ho Y, Mckay G (1998) Sorption of Dye from Aqueous Solution by Peat. Chemical Engineering Journal 70 (2):115-124

36. Robati D (2013) Pseudo-Second Order Kinetic Equations for Modelling Adsorption Systems for Removal of Lead Ions Using Multi-Walled Carbon Nanotubes. Journal of Nanostructure in Chemistry 3 (1):55

37. Weber Jr WJ, Morris JC (1963) Kinetics of Adsorption on Carbon from Solution. Journal of the Sanitary Engineering Division 89 (2):31-60

38. Vadivelan V, Kumar K (2005) Equilibrium, Kinetics, Mechanisms and Process Design for the Sorption of Methylene Blue onto Rice Husk Journal of Colloid and Interface Science 286 (1):90 - 100

39. Fierro V, Torne-Fernandez V, Montane D, Celzard A (2008). Micropor Mesopor Mat 111:276-284

40. Santhi M, Kumar P (2013) Removal Of Basic Dye Rhodamine-B By Activated Carbon-MNO_2-Nanocomposite And Activated Carbon- A Comparative Study. International Journal of Science and Research 6 (4):1968 - 1971

41. Langmuir I (1918) The Adsorption of Gases on Plane Surfaces of Glass, Mica and Platinum. Journal of the American Chemical Society 40 (9):1361 - 1403

42. Freundlich H (1906) Over the Adsorption in Solution. Journal of Physical Chemistry 57:385 - 471

43. El-Bindary AA, Abd El-Kawi MA, Hafez AM, Rashed IGA, Aboelnaga EE (2016) Removal of reactive blue 19 from aqueous solution using rice straw fly ash. J Mater Environ Sci 7 (3):1023-1036

44. Nair V, Panigrahy A, Vinu R (2014) Development of Novel Chitosan-Lignin Composites for Adsorption of Dyes and Metal Ions from Wastewater. Chemical Engineering Journal 254:491 - 502

45. Bhatt P, Vyas R, Pandit P, Sharma M (2013) Adsorption of Reactive Blue and Direct Red Dyes on Powdered Activated Carbon (PAC) - Equilibrium, Kinetics and Thermodynamic Studies. Nature Environment and Pollution Technology 12 (3):397 - 405

46. Ciobanu G, Barna S, Harja M (2016). Archives of Environmental Protection 42:3-11

47. Sayed-Ahmed S, Khalil L, El-Nabaraway T (2012). Carbon Letters 13:212-220

48. Inal M, Erduran N (2015). Polymer Bulletin 72:1735-1752

49. Banaei A, Ebrahimi S, Vojoudi H, Karimi S, Badiei A, Pourbasheer E (2017) Adsorption equilibrium and thermodynamics of anionic reactive dyes from aqueous solutions by using a new modified silica gel with 2,2 '-(pentane-1,5-diylbis(oxy))dibenzaldehyde. Chem Eng Res Des 123:50-62. doi:10.1016/j.cherd.2017.04.032

50. Asgher M, Bhatti HN (2012) Removal of reactive blue 19 and reactive blue 49 textile dyes by citrus waste biomass from aqueous solution: Equilibrium and kinetic study. Can J Chem Eng 90 (2):412-419. doi:10.1002/cjce.20531

51. Ergene A, Ada K, Tan S, Katircioglu H (2009) Removal of Remazol Brilliant Blue R dye from aqueous solutions by adsorption onto immobilized Scenedesmus quadricauda: Equilibrium and kinetic modeling studies. Desalination 249 (3):1308-1314. doi:10.1016/j.desal.2009.06.027